Volume Graphics (2007)
H. - C. Hege, R. Machiraju (Editors)

(No) More Marching Cubes

Hamish Carr †

Abstract

Isosurfaces, one of the most fundamental volumetric visualization tools, are commonly rendered using the well-known Marching Cubes cases that approximate contours of trilinearly-interpolated scalar fields. While a complete set of cases has recently been published by Nielson, the formal proof that these cases are the only ones possible and that they are topologically correct is difficult to follow. We present a more straightforward proof of the correctness and completeness of these cases based on a variation of the Dividing Cubes algorithm. Since this proof is based on topological arguments and a divide-and-conquer approach, this also sets the stage for developing tessellation cases for higher-order interpolants and for the quadrilinear interpolant in four dimensions. We also demonstrate that, apart from degenerate cases, Nielson's cases are in fact subsets of two basic configurations of the trilinear interpolant.

Categories and Subject Descriptors (according to ACM CCS): G.1.1 [Numerical Analysis]: Interpolation G.1.2 [Numerical Analysis]: Approximation I.3.5 [Computer Graphics]: Computational Geometry and Object Modeling

1. Introduction

Isosurfaces, one of the fundamental tools in visualization, extract implicit surfaces representing boundaries or features of a scalar field. Although algorithms for extracting isosurfaces have been known since the original Marching Cubes paper [LC87], isosurfaces consistent with the assumed trilinear interpolant were only recently published by Nielson [Nie03]. Unfortunately, the proof of correctness is complex, and does not generalize easily to higher dimensions and higher-order interpolants.

This paper attempts to remedy this with a straightforward proof of correctness by dividing the cube into smaller blocks, each of which has simple topology, then re-assembling the cubes to obtain the overall case. In this way, we demonstrate that no configurations other than those reported by Nielson can exist. Moreover, the techniques used in this paper are potentially useful for analysing other interpolants.

We start by reviewing Marching Cubes in Section 2, then describe the use of Finite State Machines to represent interpolant topology in Section 3. Thereafter, we will introduce in Section 4 some properties of the trilinear interpolant upon which we rely, and give an overview of our approach in Section 5. We then demonstrate that each simple block has a simple configuration in Section 6. Sections 7 to 9 then show how to subdivide into simple blocks, depending on how many body saddles exist in the interpolant, while Section 10 comments on saddles in the interpolant that fall outside the original block. Finally, Section 11 states conclusions and comments on possible future work.

2. Isosurface Extraction & Marching Cubes

Given a scalar function $T(x,y,z)$ defined over some volume of interest, an *isosurface* is the surface defined by $T^{-1}(h)$ for some *isovalue* h. Since T is usually known at a fixed set of sample points, extracting isosurfaces depends on applying an *interpolant* which defines how to compute T at points other than the original sample points. Since the sample points are commonly laid out in a cubic lattice defining a cubic mesh, one of the commonest interpolants used is the *trilinear* interpolant, defined in more detail in Section 4.

Given the cubic mesh defined by the sample points, Marching Cubes [LC87] geometrically approximates the isosurface with a separate triangulation in each cube. The function values at the cube's vertices are classified as *black* if their values are higher than the isovalue h, white otherwise. This gives $2^8 = 256$ possible cases which can be reduced by rotational or reflective symmetry to those shown in Figure 1.

The surfaces generated were, however, not watertight, a fault corrected by (among others) Montani, Scateni &

† University College Dublin

Scopigno [MSS94], whose cases were still not consistent with the (assumed) trilinear interpolant. Correcting this required consideration of saddle points on the faces of cells [NH91] and in the body [Nie03], which subdivide the cases into *configurations* - isosurfaces that share a case number but differ in their topology. Further details of the Marching Cubes literature can be found in a recent survey [NY06].

As noted above, the principal contribution of this paper is to confirm Nielson's results, but we do so by using techniques that are potentially applicable to more complex interpolants. We start by describing the use of finite state machines for modelling interpolant topology, assuming that the function values at vertices are distinct, an assumption that we can guarantee with symbolic perturbation [EM90].

3. Finite State Machines for Interpolant Modelling

For a given cube, consider a sweep from high to low isovalues. Each vertex starts off as white (lower than h), then becomes black (higher than h). Thus, each cube uses a sequence of different cases dictated by the order in which the vertices are swept past. This sequence can be represented [CS07] by a finite state machine for geometric and topological computations. To construct the finite state machine for a particular interpolant or set of cases, we define the states to be the cases, and add a transition from each state (case) to each other case with one extra black vertex.

Figure 1 shows the finite state machine for watertight Marching Cubes cases [MSS94]. Each cube always starts with case 0, then sweeps to case 1, then to case 2, 3 or 4. But, with two black vertices each, case 2 never sweeps to case 3 or 4. Instead, case 2 may sweep to cases 5 or 6, but not 7, since case 2 has two edge-adjacent black vertices and case 7 has no edge-adjacent black vertices. And so forth, until the full finite state machine is constructed. We will use this representation to impose indirect constraints on the possible configurations of the trilinear interpolant.

4. The Trilinear Interpolant

Trilinear interpolation repeats linear interpolation with respect to the x, y and z axes sequentially. Thus, for values $T_{000}, T_{001}, T_{010}, T_{011}, T_{100}, T_{101}, T_{110}, T_{111}$ at the vertices of the cube $[0,1]^3$, the trilinear interpolant is [Nie03]:

$$\begin{aligned} T(x,y,z) &= axyz + bxy + cyz + dxz + \\ &\quad ex + fy + gz + h \qquad (1) \\ a &= T_{111} - T_{110} - T_{101} - T_{011} + \\ &\quad T_{100} + T_{010} + T_{001} - T_{000} \\ b &= T_{110} - T_{100} - T_{010} + T_{000} \\ c &= T_{011} - T_{010} - T_{001} + T_{000} \\ d &= T_{101} - T_{100} - T_{001} + T_{000} \\ e &= T_{100} - T_{000} \\ f &= T_{010} - T_{000} \\ g &= T_{001} - T_{000} \\ h &= T_{000} \end{aligned}$$

Saddle points exist where the gradient is zero, i.e. where all three partial derivatives are zero [Nie03]:

$$\frac{\delta T}{\delta x} = ayz + dz + by + e = 0 \qquad (2)$$

$$\frac{\delta T}{\delta y} = axz + cz + bx + f = 0 \qquad (3)$$

$$\frac{\delta T}{\delta z} = axy + cy + dx + g = 0 \qquad (4)$$

Equations 3 and 4 can be solved for y, z in terms of x and substituted into Equation 2 to obtain [Nie03]:

$$x = \frac{1}{a}\left[-b \pm \sqrt{-\frac{a_y a_z}{a_x}}\right] \qquad (5)$$

$$y = \frac{1}{a}\left[-c \pm \sqrt{-\frac{a_x a_z}{a_y}}\right] \qquad (6)$$

$$z = \frac{1}{a}\left[-d \pm \sqrt{-\frac{a_x a_y}{a_z}}\right] \qquad (7)$$

$$\begin{aligned} a_x &= ae - cd \\ a_y &= af - bd \\ a_z &= ag - bc \end{aligned}$$

Equations 5-7 are dependent on each other, and there are at most two distinct body saddles with distinct isovalues:

$$\begin{aligned} s &= m \pm \vec{v} \qquad (8) \\ m &= \frac{1}{a}(-c, -d, -b)) \\ \vec{v} &= \frac{1}{a}\left(\sqrt{-\frac{a_y a_z}{a_x}}, \sqrt{-\frac{a_x a_z}{a_y}}, \sqrt{-\frac{a_x a_y}{a_z}}\right) \end{aligned}$$

Both *midpoint* m and vector $\vec{v}$ affect our analysis. Moreover, the components of v are interdependent, so $v_x = 0$ if and only if $v_y = v_z = 0$, and two distinct saddles s_u, the *upper* and s_l, the *lower saddle*, have isovalues $u > l$ respectively.

Linear changes of variable move isosurfaces in domain or in range. $L(x) = p + qx$ scales and translates along the x-axis so that $L(m) = (p + m_x, m_y, m_z)$ and $\vec{v} = (qv_x, v_y, v_z)$, i.e. the location of the midpoint is translated and the locations of the saddles are scaled and translated along the $x-$ axis.

Setting $p = 1$ and $q = -1$ reflects the interpolant and pairs of isovalues along x-aligned edges. Since this also applies to the $y-$ and $z-$ axes, we can therefore assume that $v_x, v_y, v_z > 0$, and that the development of isosurfaces occurs along the line $m + \vec{v}t$. We can then force the upper saddle to be $s_u = m - \vec{v}$ and the lower saddle $s_l = m + \vec{v}$ by inverting $\vec{v}$ and reflecting along all three axes.

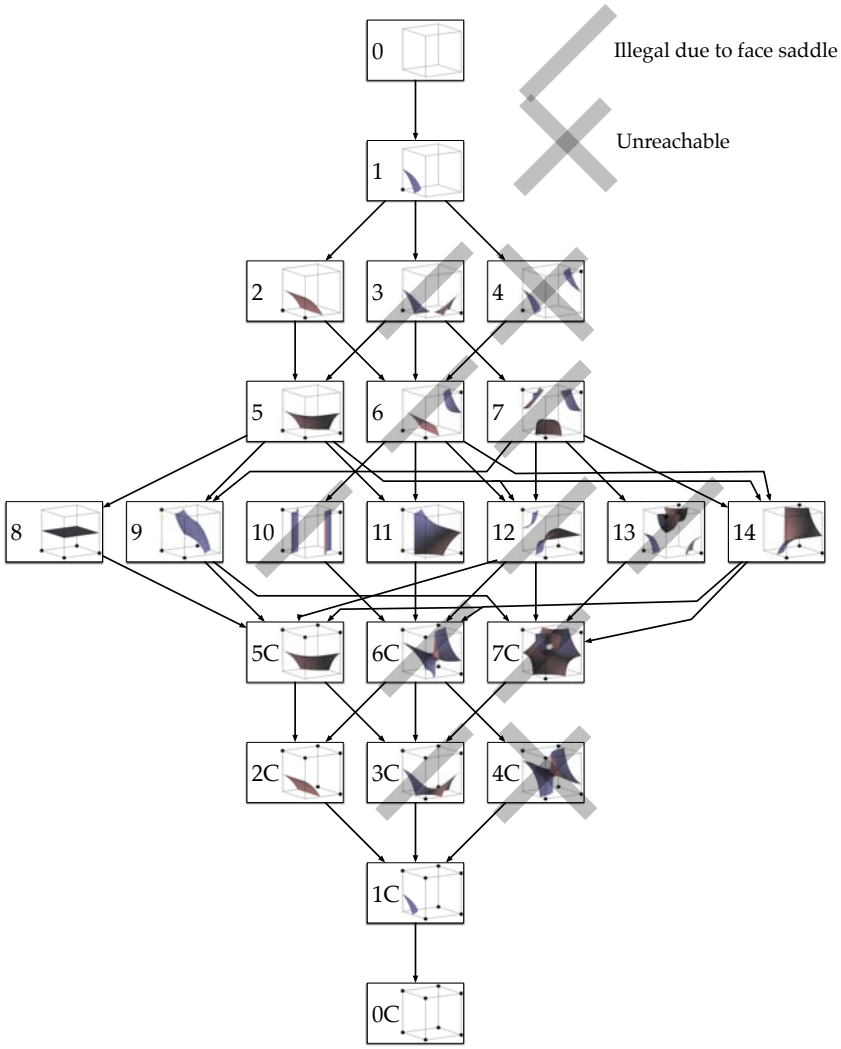

Figure 1: *Isosurface evolution of crackfree Marching Cubes [MSS94], represented as a finite state machine [CS07]. Not all cases exist in a simple block. Note that Case 4 must be followed by Case 6, implying the existence of a face saddle in the block.*

4.1. Cross-Gradients on Midpoint Lines

We will also exploit the uniformity of gradients perpendicular to *midpoint lines* - axial lines $x = -\frac{b}{a}, y = -\frac{c}{a}$, or $z = -\frac{d}{a}$ through the midpoint m. Note that $\frac{\delta T}{\delta x}$ is independent of x in Equation 2 and is linear in z for a given y value. For $y = -\frac{c}{a}$:

$$\frac{\delta T}{\delta x} = a(-\frac{d}{a})z + dz + b(-\frac{d}{a}) + e \quad (9)$$

$$= -dz + dz - (\frac{bd}{a}) + e \quad (10)$$

$$= \frac{a_x}{a} \quad (11)$$

It follows that the gradient *perpendicular* to a midpoint line is constant along that line.

5. Overview of Case Construction

To show that Nielson's cases are complete and correct, we will divide each cube into *blocks* - axis-aligned rectilinear subsets or supersets of the cube. Instead of dividing equally [CLL*88], we use planes that guarantee *simple blocks* - blocks which only have body or face saddles at their vertices. Section 6 shows that such *simple blocks* contain a single surface homeomorphic to a sheet. Section 7 then constructs the cases where Equation 8 has two solutions by defining an ordering of the subblocks' vertices, then using this to construct finite state machines showing the development of cases in the cube. Similarly, Section 8 will deal with cubes with one saddle, while Section 9 will deal with cubes with no saddle, and Section 10 deals with saddles outside the initial cube.

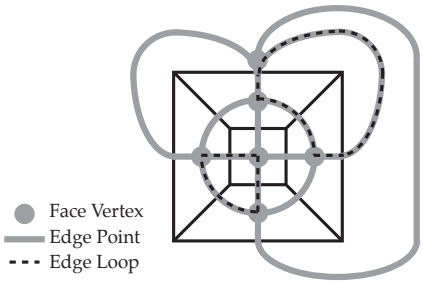

Figure 2: *Dual Graph of Simple Block, showing edge loops. Since linearity precludes multiple loops intersecting an edge, and lack of face saddles precludes multiple loops intersecting a face, only one configuration is possible: base case 4C, which we know to be impossible.*

6. Handling Simple Blocks

We will show that a simple block B has isosurfaces that must intersect faces of B, that cases 3, 4, 6, 7, 10, 12, & 13 and their complements imply the presence of face or body saddles, and that each remaining case has a single surface that is homeomorphic to a sheet (i.e. without handles).

Lemma 1 Each surface in block B intersects some face of B.

Proof: Assume not. Then there is a surface C entirely contained in the interior of B. As a contour of a continuous function, it is a closed surface with non-empty interior. Draw an axis-parallel line through any point in this surface's interior. This line must intersect the surface in at least two points, which therefore have the same isovalue. Since the trilinear interpolant on an axis-parallel line is linear, all points on this line have the same isovalue, including the points at which the line intersects the boundary of the cell. □

Lemma 2 Cases 3, 4, 6, 7, 10, 12, 13, 7C, 6C, 4C and 3C may not occur in a simple block.

Proof: Since simple blocks have face saddles only at their vertices, they may not have ambiguous faces with two diagonally opposed black vertices and two diagonally opposed white vertices, as the (bilinear) interpolant on such a face would have a saddle point [NH91]. Since cases 3, 6, 7, 10, 12, 13, 7C, 6C and 3C all have ambiguous faces, they cannot occur in a simple block. Moreover, since case 4 must always be followed by case 6, which has an ambiguous face, case 4 cannot occur either, and similarly, case 4C cannot occur. □

Lemma 3 Each isosurface in a simple block B is connected (i.e. it has only one contour).

Proof: Suppose not. Then there exist at least two disjoint surfaces. By Lemma 1, these surfaces each intersect the faces of B in *edge loops* connecting one edge to another [NH91]. Since none of the faces are ambiguous, no face can have more than one edge loop and the cycles are disjoint. Only one set of two edge loops is then possible, as shown in Figure 2. But this describes base case 4 or 4C, which cannot occur in a simple block. □

Theorem 4 Every isosurface in a simple block B is homeomorphic to a sheet.

Proof: For reasons of space, we give an outline only. Suppose not. There must be a highest isovalue at which the surface increases genus, which may only happen at a point that is locally a saddle point p at which two isosurfaces meet. This point may be in the interior, on a face, on an edge, or at a vertex. **Interior:** p must therefore be a body saddle, which cannot happen in a simple block. **Face:** if either of the two isosurfaces fails to intersect the face, p must again be a body saddle. So both isosurfaces intersect the face, and p is then a face saddle, which cannot happen in a simple block. **Edge:** if either isosurface is interior, p must be a body saddle, so both intersect adjacent faces. But, with two adjacent (non-ambiguous) faces, each must be on a different face, and p must be a body saddle. only remaining possibility is that the point is at a vertex of the cube, and a contradiction can be established in this case based on monotone paths. □

Corollary 5 In a simple block B, every isosurface is of case 0, 1, 2, 5, 8, 9, 11, 14, 5C, 2C, 1C, or 0C, and the standard triangulations [LC87,MSS94] for these cases are topologically equivalent to the correct contours.

7. Blocks with Two Body Saddles

We know from Equation 5 that there may be zero, one or two body saddles. We consider each possibility separately, divide non-simple blocks into multiple simple blocks, then use finite state machines to examine the sequence of cases. For simplicity, we assume that all body saddles are inside the block until Section 10.

If there are two body saddles, we divide the cube into simple blocks with axis-perpendicular planes passing through each saddle, as shown in Figure 3. From Section 4, we know that the two saddles s_u and s_l have distinct isovalues $u > l$, and that $v_x, v_y, v_z > 0$ with s_u closer to $(0,0,0)$ than s_l.

We thus divide the cube into the blocks defined by the planes $x = 0, x_u, x_l, 1$, $y = 0, y_u, y_l, 1$, $z = 0, z_u, z_l, 1$, where $(x_u, y_u, z_u) = (p_x - v_x, p_y - v_y, p_x - v_z)$ and $(x_l, y_l, z_l) = (p_x + v_x, p_y + v_y, p_x + v_z)$. These planes define a set of points (vertices - various colours), a set of lines (green), and sub-blocks. We will use T_{ijk} to refer to the isovalue at vertex (i, j, k), where $i, j, k \in \{0, u, l, 1\}$ For example, the isovalue of the upper saddle can be written as T_{uuu}, while the isovalue of the adjacent vertex in the $+z$ direction will be T_{uul}. Moreover, each line is axis-parallel and therefore linear in T.

Now, the trilinear interpolant is linear along axis-parallel lines, and at a body saddle, $\frac{\delta T}{\delta x} = \frac{\delta T}{\delta y} = \frac{\delta T}{\delta z} = 0$. Since each partial derivative is the slope of T along an axis-parallel line T is constant on these lines, and all points co-axial with a saddle have the same isovalue.

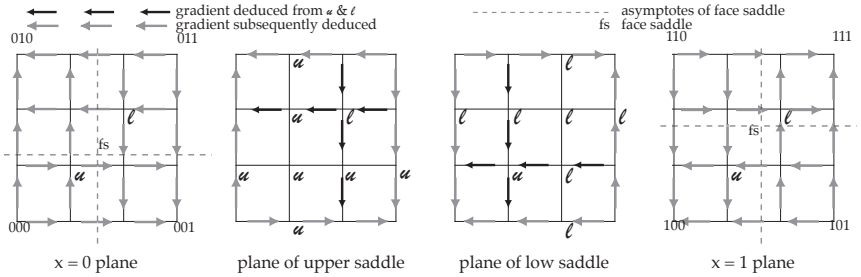

Figure 4: *Ordering of Sub-block Vertices, shown as a set of planes. Arrows show the direction of ascent. Note that face saddles may only occur in the central subblock on each face.*

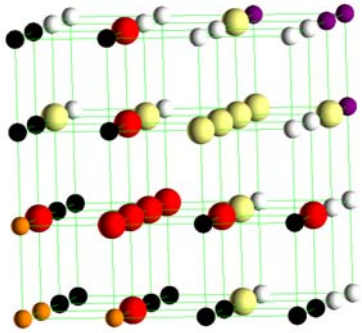

Figure 3: *Subdivision of Block with Two Saddles. Broadly speaking, darker colours have higher isovalues, lighter colours have lower isovalues. Red indicates vertices with the same isovalue u as the upper saddle, yellow indicates vertices with the same isovalue l as the lower saddle. Otherwise, vertices of the same colour need not share an isovalue - black implies an isovalue higher than u, purple is higher than l, orange is lower than u, white is lower than l.*

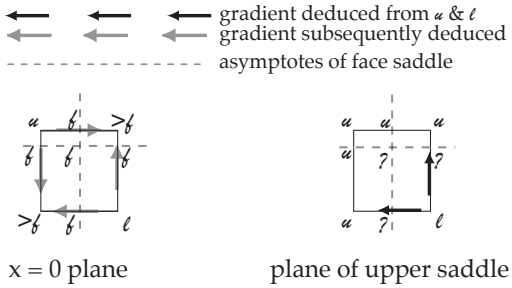

Figure 5: *Ordering of Sub-block Vertices for Face Block. Extra vertices are added to the central face of the $x = 0$ plane and the plane of the upper saddle, and their vertex ordering fixed. Vertices marked '?' have values between l and u.*

Coding the upper and lower saddle isovalues u and l as red and yellow, we extend them as shown, then consider cross-gradients. A line with one red and one yellow then has known ordering (black is greater than u, white is lower than l). Similarly, we can identify the purple vertices as above l but known to be above u, and the orange vertices as below u but not known to be below l. These relationships are easier to see on the individual planes shown in Figure 4: the initial values of u and l allow us to deduce first the black gradients on lines, then the grey gradients on the remaining lines.

Now consider the $x = 0$ face shown at the left of Figure 4. We know that ambiguous faces only occur when two diagonal vertices are both higher than the remaining two vertices. As we can see from the figure, this can only happen in the central subface, where u and l are known to be lower than the two remaining values. Moreover, none of the remaining subfaces on *any* of the planes has this configuration. It then follows that the central subblock on each face has one face saddle and no other subblock has any face saddles.

7.1. Cases for the Face Block

As an example, we now construct the finite state machine for this face block. We deal with the face saddle by subdividing the face block into four simple blocks by passing planes through the face saddle perpendicular to the face. Since the face saddle has zero gradient on the face, the added vertices on the $x = 0$ have the same isovalue f as the saddle. And the additional points on the plane of the upper saddle will have values between u and l, as shown in Figure 5. Since none of the subfaces thus constructed are ambiguous, we know that the subblocks are simple blocks. Moreover, the constraints marked in Figure 5 impose severe constraints on the cases that may occur in which order, as shown in Figure 6.

Only vertices $0ul$ and $0lu$ have isovalues $> f$, as marked, so a sweep starts as case 0 in each sub-blocks, then sweeps past $0ul$ or $0lu$, generating case 1 in one sub-block and case 0 in the other three, giving an overall case 1 in either case. We then sweep past the other of $0lu$ and $0ul$, generating Niel-

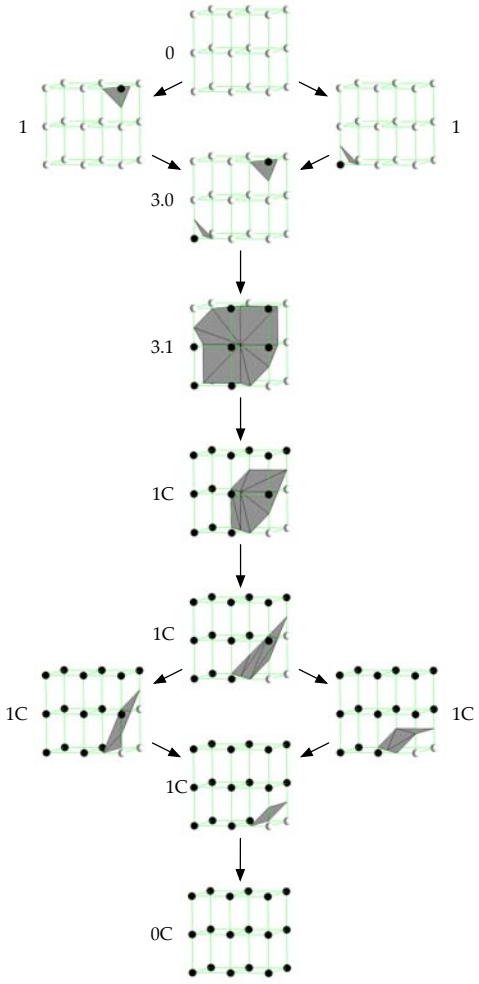

Figure 6: *Cases Possible for Face Block. Note how the sequence of cases in individual simple blocks can be used to build up non-simple cases such as 3.1.*

son's case 3.0, in which two separate surfaces appear. We next sweep past f, and get case 5 in two subblocks, case 8 in the other two, generating case 3.1, in which a single tent-like surface appears. The next isovalue swept past is u, giving cases 1C, 2C, 2C and 5, generating case 1C overall. Finally, although the cases in individual sub-blocks change, we generate case 1C until case 0C is reached.

We now ignore the additional vertices inserted and observe that this block uses cases 0, 1, 3.0, 3.1, 1C and 0C, with the face saddle being used to disambiguate between cases 3.0 and 3.1 as in the Asymptotic Decider [NH91]. Moreover, each of the three face blocks which includes the upper saddle uses this sequence of cases, while the remaining three use the complementary cases.

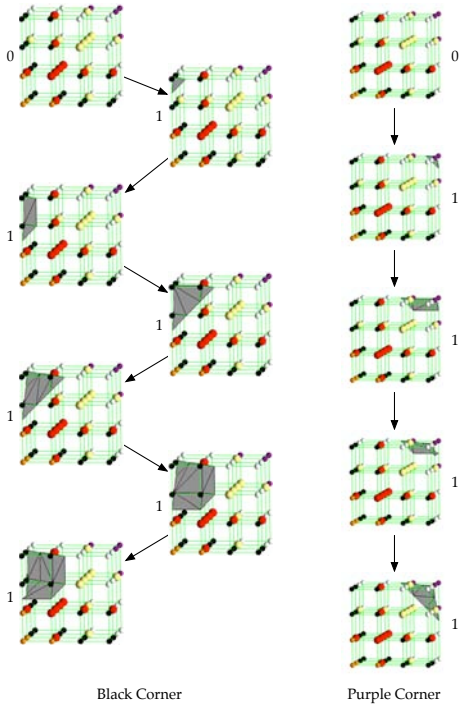

Figure 7: *Left: Sample Evolution Near Black (High) Corner. Right: Evolution of Surfaces near Purple (High) Corner. Case Numbers are those used by Nielson [Nie03].*

7.2. Cases at High-Isovalue Corners

We now turn our attention to the entire block. In our isovalue sweep, we note that the three black corners have isovalues higher than either saddle, while the purple corner of the block must have isovalues higher than the lower saddle, but may or may not have isovalues higher than the upper saddle. At a black corner such as 100, the sequence (subject to symmetries) is as shown in Figure 7. Given our constraints from Figure 4, the corner itself is swept first, then each of its immediate neighbours

Let us begin by considering the evolution of a surface at one of the black corners, e.g. corner 100, as shown in Figure 7. The constraints in Figure 4 require that the first vertex swept past is the corner. Moreover, the red, yellow, orange and white vertices are all at lower isovalues than all black vertices, so the surface must connect across the face saddles to the adjacent black corners before the surface may sweep through the higher (red) saddle. Consequently, the local development at the corner is that shown in Figure 7 until connections at face saddles occur, subject to minor variations in the order in which vertices are swept past.

Similarly, as shown in Figure 7, development at the purple corner of the block is strongly constrained by the yellow,

orange and white vertices known to have lower isovalues, and by the constraints shown in Figure 4. Consequently, the development of the surface follows the progression shown in Figure 7, subject to symmetries.

7.3. Overall Evolution in Block

Now that we have analysed the behaviour of the surfaces near each corner and at each face saddle, we can develop the set of cases swept through by the isosurface in the full block - Figure 8 shows the evolution possible, with Figure 9 showing the surfaces in the first few states. Note that the transition from 7.3.0 to 9 involves sweeping past the orange vertices at the near corner of the block, but this is just the inverse of the case shown in Figure 7, as these vertices have isovalues lower than the upper saddle.

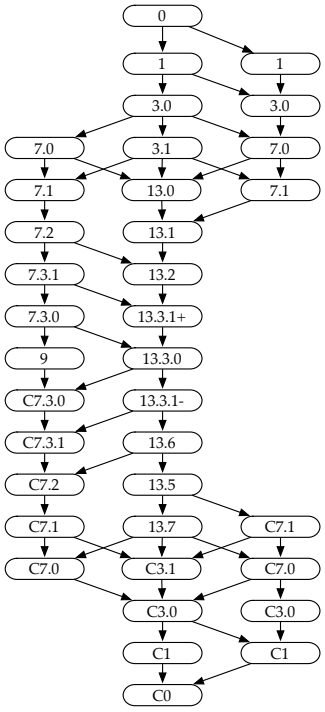

Figure 8: *Finite State Machine In Block with Two Body Saddles. See Figure 9 for surfaces in first few states. Case (state) numbers as in Nielson [Nie03].*

8. One Body Saddle

In the previous section, we showed which cases are possible when two body saddles exist in the block. One body saddle can occur in one of two ways: either there can be only one solution to Equation 8 (i.e. $\vec{v} = \vec{0}$), or there can be two saddles, only one of which occurs inside the block.

If there is only one solution, then $\vec{v} = \vec{0}$, and the midpoint m is the body saddle. Recall from Section 4.1 that the partial derivatives perpendicular to the midpoint lines are constant. Since the three partial derivatives at the body saddle are known to be zero, it follows that the partial derivatives to the midpoint lines are also zero. Moreover, the trilinear function is linear on axis-parallel lines in the midpoint planes. Thus, each line perpendicular to a midpoint line has zero gradient along it, and it follows that every point in each midpoint plane has the same function value as m, the saddle point. In particular, if we split the block along the midpoint planes, all vertices of sub-blocks except the original vertices of the block will have function value T_{mmm}.

However, by assumption, the vertices of the original block are unique. Thus, at least one of them has a function value other than T_{mmm} - without loss of generality, $T_{000} < T_{mmm}$. Since $T_{0m0} = T_{mmm}$, the gradient along the line $y = 0$ is positive, so $T_{010} > T_{mmm}$, as are T_{001} and T_{100}. Continuing in this fashion, we find that all vertices of the block with even parity are below the saddle, while all vertices of odd parity are above the block. Each sub-block then has 7 vertices at T_{mmm} and 1 that is either above or below - as a result, only cases 0, 1 or 1C and 0C are possible. Combining the sub-blocks, only cases 0, 1, 3.0, 7.0, 13.0 and their complements are possible.

9. No Body Saddles

It is possible for there to be no body saddles in the block either because there are no body saddles (no real roots of Equations 5-7), or because there are body saddles which simply do not occur in the block, in which case, as in Section 8, we have subsets of the surfaces developed for one or two body saddles. We therefore concentrate on the case where no such body saddles exist anywhere. The analysis will follow the pattern broadly set out above: first, we will subdivide the block to constrain the possible face saddles, then establish an ordering, then consider the evolution in each sub-block, then reassemble the sub-blocks to obtain the overall evolution.

We first note that, even where there are no body saddles, the point $m = (\frac{-c}{a}, \frac{-d}{a}, \frac{-b}{a})$ is still well-defined in Equation 8 unless $a = 0$ (the degenerate case). If m is not in our block, we can use use linear transformations to scale the block to include m. Without loss of generality, therefore, we assume that m is in the block, and split the block with axis-perpendicular planes through m. Moreover, since we know that we can add or subtract a constant to all isovalues without changing the fundamental topology, we assume that $T_{mmm} = 0$.

As with the two body saddle case, our next task is to set up inequalities that constrain the possible cases. We recall from Section 4.1 that the gradients along the midpoint lines are constant, and equal to $\frac{a_x}{a}$, $\frac{a_y}{a}$ and $\frac{a_z}{a}$. Since the discriminant in Equations 5 to 7 is negative when no saddles exist, it follows that none of a_x, a_y or a_z may be zero, and that therefore the partial derivatives at m are non-zero. Without loss of

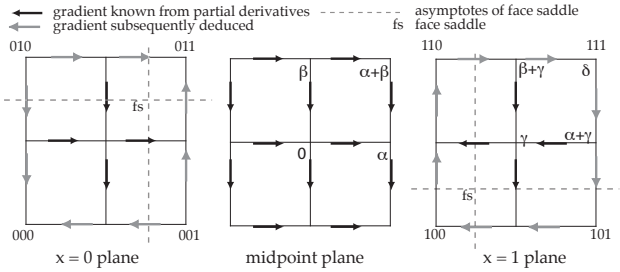

Figure 10: *Ordering of Vertices in No Body Saddle Case. The partial derivatives at the midpoint are guaranteed to be non-zero and are assumed to be positive. From Section 4.1, we also know the partial derivatives at the ends of the midpoint lines. See text for balance of development*

generality, we assume that they are all positive - if not, we merely apply a reflection to that axis to reverse the direction.

Moreover, the partial derivatives perpendicular to the midpoint lines are constant, so we know the partial derivatives at the ends of the midpoint lines. Let the function values at the positive ends of these lines be $\alpha, \beta, \gamma > 0$, as marked in Figure 10. Since the lines passing through these points have the same gradient as those passing through the midpoint, we can easily determine the values $\alpha+\beta$, $\alpha+\gamma$ and $\beta+\gamma$ marked in the figure. We next observe that these points define a sub-block, of which only the isovalue δ is not known relative to the others. We evaluate Equation 5 for this sub-block, and obtain (derivation omitted):

$$\begin{aligned} a' &= \delta-\alpha-\beta-\gamma \\ a'_x &= \alpha a' \\ a'_y &= \beta a' \\ a'_z &= \gamma a' \end{aligned}$$

Since the discriminant under the square root sign must be negative, we know that:

$$-\frac{\alpha a' \beta a'}{\gamma a'} < 0$$

and since we know that $\alpha, \beta, \gamma > 0$, it follows that:

$$\begin{aligned} a' &> 0 \\ \delta-\alpha-\beta-\gamma &= 0 \\ \delta &> \alpha+\beta+\gamma \\ \delta &> \alpha+\beta, \alpha+\gamma, \beta+\gamma \end{aligned} \qquad (12)$$

which gives us three additional gradients, plus three symmetrically computed gradients at 000.

Subject to symmetry, the only remaining relationship to be considered is that between 101 and 100. This may point in either direction, but we can force $T_{101} < T_{100}$. T increases by $\delta-(\alpha+\gamma) > \beta$ from $1m1$ to 111, but only by *beta* from

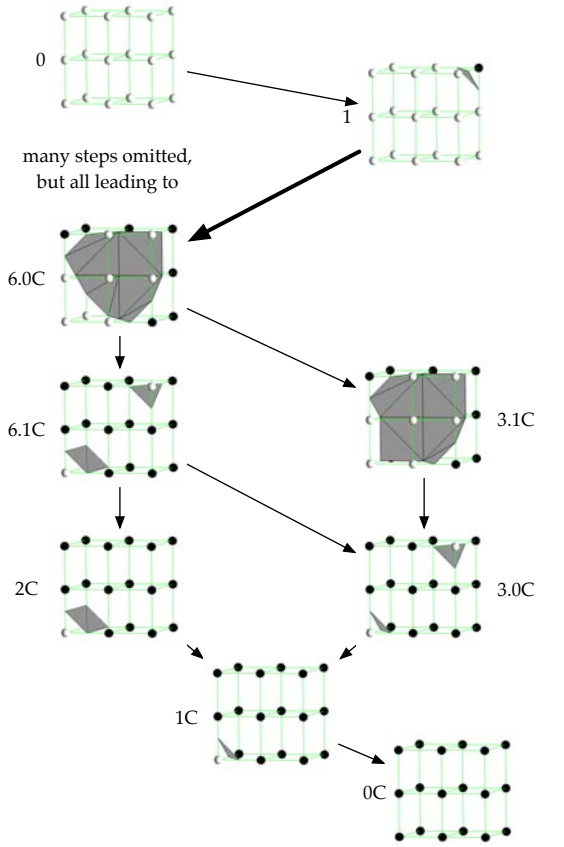

Figure 11: *Block with Face Saddle in No Body Saddle Case. Although following the individual cases is tedious, the evolution at the face saddle is resolved by the evolution in the subblocks.*

$1mm$ to $11m$. Thus, following backwards through 101 and $10m$, eventually we will find points $(1,y,1)$ and $(1,y,m)$ for which $T(1,y,1) < T(1,y,m) < T(1,y,0)$. We therefore move the boundary of the block outwards until this is satisfied: all other inequalities determined so far are unchanged. Repeating this up to six times, one for each face of the block, we see that we are guaranteed that our block is contained within some block for which all of the inequalities shown hold.

We note that face saddles can occur only in the faces marked, guaranteeing that no more than one face saddle, and no body saddle, may occur in each sub-block. Repeating the process in Section 7.1, we end up with Figure 11 or its converse as the evolution in six of the sub-blocks, and a simple evolution in the two remaining blocks.

Finally, we again assemble the individual sub-blocks, and discover that, subject to symmetry and to the detailed ordering of the vertices, the evolution if no body saddles are present follows the sequence shown in Figure 12.

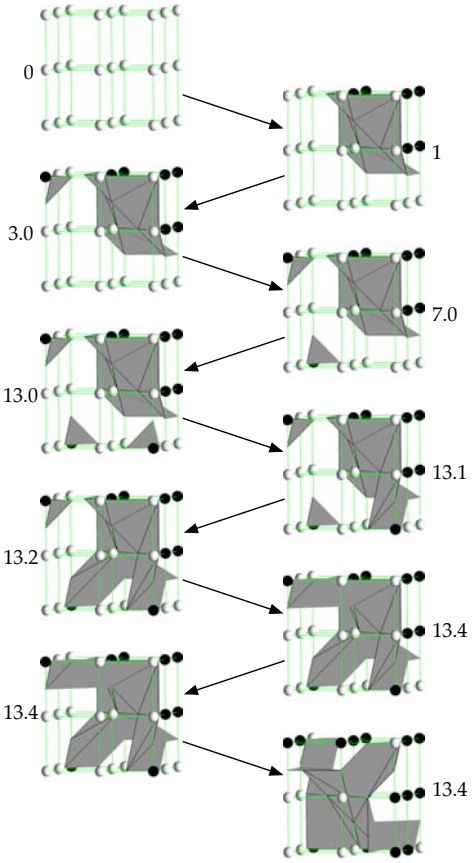

Figure 12: *Example of Overall Evolution in No Saddle Case. Once the bottom case is reached, the sequence reverses.*

10. Saddles Outside Block

In the above, we assumed that all body saddles were inside the block. This is not always the case, but can be handled by expanding the block to include all body saddles - the cases used are then subsets of the cases shown above. Detailed analysis follows the same pattern as above - establishing inequalities to constrain vertices, dividing into simple blocks, and building up the result from simple blocks.

Ultimately, all of the cases presented by Nielson [Nie03] were encountered and no others.

11. Conclusions & Future Work

We have established that Nielson's configurations are complete and correct. Moreover, we have shown that there are two basic possibilities for the development of isosurfaces in the cell, involving two body saddles and no body saddles, respectively, plus one (degenerate) case with one body saddle, and observed that all other possibilities are merely subsets of these. We have also built up a set of techniques - division into simple blocks, constraint by inequalities, and reconstruction from simple blocks. We believe that these techniques will significantly ease the task of determining tessellation cases for higher order interpolants and for the quadrilinear interpolant.

While the proof shown should in principle be usable for tessellation, the division of each cube depends on the body saddles of that cube. In practice, this means that triangulated approximations in adjacent cells will show cracks similar to the original Marching Cubes. We believe that this can be remedied by adjustments on the faces of the cubes, and that this will allow high-quality approximations of the correct trilinear surface.

12. Acknowledgements

Acknowledgements are due to University College Dublin and Science Foundation Ireland for supporting this research, and to the reviewers.

References

[CLL*88] CLINE H. E., LORENSON W. E., LUDKE S., CRAWFORD C., TEETER B.: Two algorithms for the three-dimensional reconstruction of tomograms. *Medical Physics 15*, 3 (1988), 320–327.

[CS07] CARR H., SNOEYINK J.: Representing interpolant topology for contour tree computation. In *TopoInVis 2007 (Grimma)* (2007).

[EM90] EDELSBRUNNER H., MÜCKE E. P.: Simulation of Simplicity: A technique to cope with degenerate cases in geometric algorithms. *ACM Transactions on Graphics 9*, 1 (1990), 66–104.

[LB03] LOPES A., BRODLIE K.: Improving the robustness and accuracy of the marching cubes algorithm for isosurfacing. *IEEE Transactions on Visualization and Computer Graphics 9*, 1 (2003), 16–29.

[LC87] LORENSON W. E., CLINE H. E.: Marching Cubes: A High Resolution 3D Surface Construction Algorithm. *Computer Graphics 21*, 4 (1987), 163–169.

[MSS94] MONTANI C., SCATENI R., SCOPIGNO R.: A modified look-up table for implicit disambiguation of Marching Cubes. *Visual Computer 10* (1994), 353–355.

[NH91] NIELSON G. M., HAMANN B.: The Asymptotic Decider: Resolving the Ambiguity in Marching Cubes. In *Proceedings of Visualization 1991* (1991), IEEE, pp. 83–91.

[Nie03] NIELSON G. M.: On Marching Cubes. *IEEE Transactions on Visualization and Computer Graphics 9*, 3 (2003), 283–297.

[NY06] NEWMAN T. S., YI H.: A survey of the marching cubes algorithm. *Computers And Graphics* (2006), 854–879.

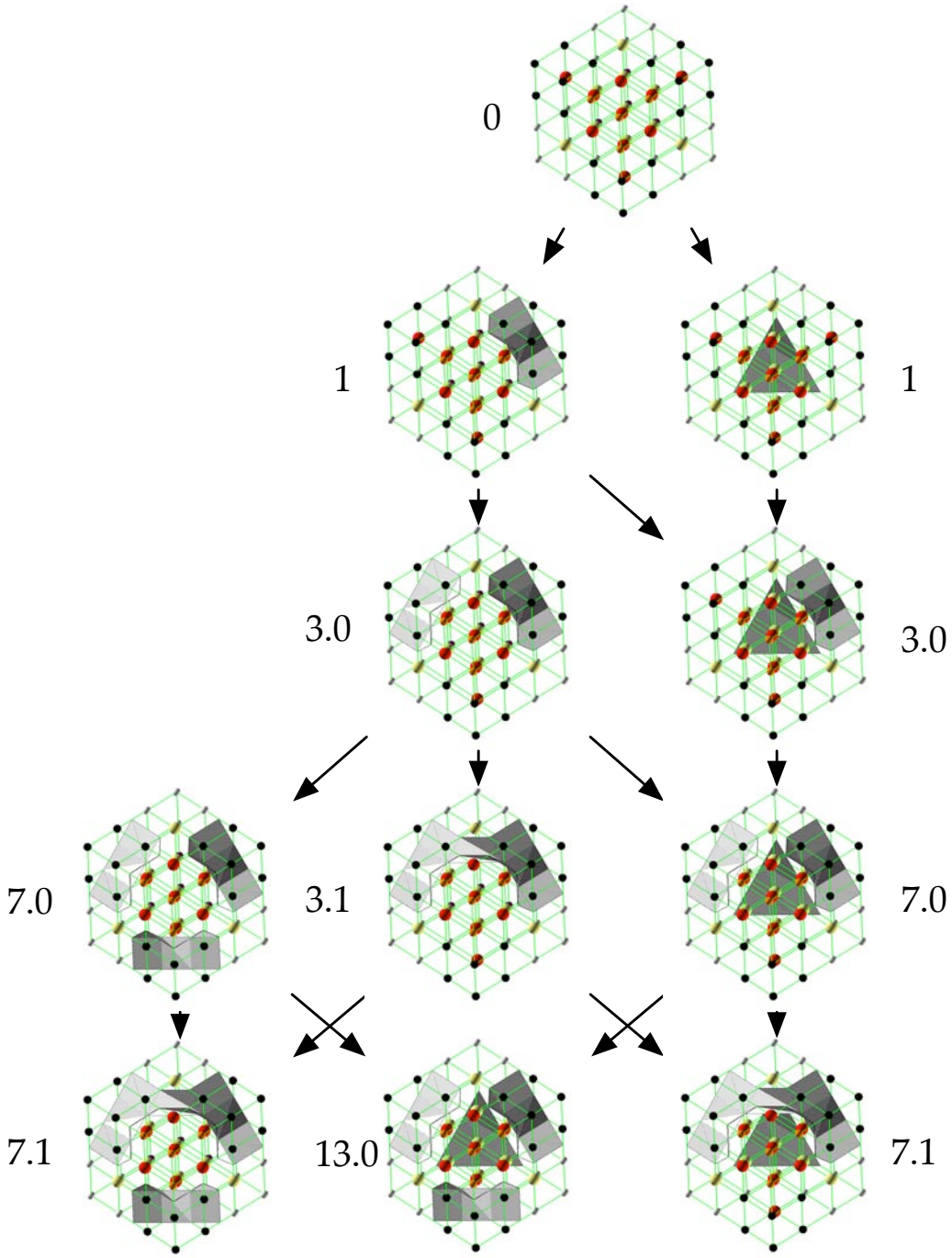

Figure 9: *Partial Development of Surfaces In Block with Two Body Saddles. The surface at the far (purple) corner develops independently for all isovalues greater than that of the lower (yellow) saddle. The surfaces at the remaining high (black) vertices are swept past one at a time in accordance with Figure 7. Note how constrained the sequence of cases is, as all black vertices must be swept past before the high (red) body saddle may be swept past. Only part of the finite state machine is shown with surfaces.*